

## Upper limits on emission of neutrons from Ti in pressurized D<sub>2</sub> gas cells: A test of evidence for “cold fusion”

S. L. Rugari, R. H. France, B. J. Lund, S. D. Smolen, Z. Zhao, and M. Gai  
*A. W. Wright Nuclear Structure Laboratory, Yale University, New Haven, Connecticut 06511*

K. G. Lynn

*Department of Physics and Applied Science, Brookhaven National Laboratory, Upton, New York 11973*

(Received 31 May 1990)

We have used a low background detector with high efficiency for detection of bursts to search for emission of neutrons from Ti alloy in pressurized D<sub>2</sub> gas cells (cooled to 77 K in liquid nitrogen). Each cell contained between 16 and 67 g of Ti alloy chips and was prepared by methods identical to those used in a recent Los Alamos-Brigham Young University collaboration of Menlove *et al.* Three to four cells were used in each experimental run, with a total counting time of 103 h, leading to an estimate (based on the early reports of Menlove *et al.*) of at least four bursts and as many as 12 bursts expected in our experiment. In a later report the burst rate of Menlove *et al.* is greatly reduced leading to only one or so burst(s) expected in our experiment. The data were analyzed in two modes. In the first mode (singles mode) all detectors were used to search for neutron bursts with an efficiency of 28% for neutron detection and a background of 100 counts per hour (cph). In the second mode (coincidence mode) the neutron time of flight was measured in a search for random emission with an efficiency of 2% and a background of 2 cph. No statistically significant deviations from the background were observed for correlated neutrons emitted in bursts or for neutrons emitted randomly. All events are shown (with 90% confidence) to be consistent with background. For bursts of neutrons we deduce (with 90% confidence) an upper limit on the bursts' size of 50 neutrons. Our upper limit on the random emission of neutrons, 0.008 *n*/sec (90% confidence), is a factor of 6 to 25 smaller than the range of rates for random emission above background reported by the Los Alamos-Brigham Young University collaboration.

### I. INTRODUCTION

Recent evidence for “cold fusion”<sup>1</sup> was reported by Menlove *et al.* in a Los Alamos-Brigham Young University experiment,<sup>2</sup> where bursts of 50–300 neutrons (measured over a 100  $\mu$ sec period) were reported from pressurized D<sub>2</sub> cells containing Ti alloy chips (“dry cells”). The cells were cooled to liquid nitrogen temperature and, while warming up, were placed in front of the Los Alamos neutron detection system which consists of twelve <sup>3</sup>He counters with a total efficiency of  $\epsilon=30\%$ . In Ref. 2 it is also stated that most of the bursts were observed about 30–40 min into the warm up cycle at a cell temperature of  $-30^\circ\text{C}$ , but some of the neutron bursts were also observed at room temperature. In addition, in Ref. 3 it is reported that *only 5%* of the running time was spent while the cells were warming up, and in Ref. 4 it is reported that *only 2%* of the running time was spent while the cells were warming up, at temperatures where it is reported that most of the neutron bursts were observed. Consequently, while the experimental study reported here is much shorter (spanning some 10 days), the time spent in our experiment while the cylinders are warming up (22% of the total running time) corresponds to a large fraction of that of Refs. 2–4 (see Appendix C).

Bursts of neutrons were searched for using six such “dry cells” with characteristics essentially identical to

those used in the Los Alamos experiment.<sup>2–4</sup> Three to four cylinders were placed in the detector system during each experiment. We report here the experimental procedure and results of our experiment. The results show no statistically significant deviations from the background for correlated neutrons emitted in bursts or for neutrons emitted randomly.

Our detector system consists of twelve NE213 liquid scintillator neutron detectors<sup>5</sup> that can be operated in two main modes: in singles mode with high total efficiency ( $\epsilon=28\pm 5\%$ ) and a moderate background (rate=100 counts per hour), or in coincidence mode with a moderate total efficiency ( $\epsilon=2\pm 1\%$ ) and with low background [rate = 2 counts per hour (cph)]. Additional tests of other “dry cells” fabricated in Brookhaven National Laboratory were also conducted in this search with similar results obtained and reported here.

### II. EXPERIMENTAL PROCEDURES

#### A. Ti samples

The “dry cells” used in this experiment contained between 16–67 grams (each) of Ti662 (Ti with 6% Al, 6% V, and 2% Sn) filings provided by S. E. Jones and were pressurized to 40–60 atmospheres of D<sub>2</sub> gas. An additional four cylinders contained material from

Brookhaven National Laboratory. The cylinders were cooled in liquid nitrogen to 77 K and then allowed to warm up to room temperature. Three to four cylinders were used in each experiment as listed in Table I, where we specify the experiments performed. In Table II we specify the cylinders and the details of the Ti material used in each run.

The majority of the data were obtained from cylinders 1, 2, 3, 4, 6, and 8, which are identical to the ones used in Refs. 2-4. The actual cylinders were provided by S. E. Jones and are the same cylinders as those used by the Los

Alamos-BYU collaboration. They are 23 cm long, have a 2.5 cm inner diameter and a 4.5 cm outer diameter, with the exception of cylinder 4, which was smaller than the others.

The cells were prepared by S. E. Jones according to procedures developed in the Los Alamos-BYU collaboration as follows:

- (1) The Ti662 filings were washed in  $\text{CH}_2\text{Cl}_2$  and methanol.
- (2) The Ti662 filings were dried in air.
- (3) The Ti662 filings were loaded into the cylinders.

TABLE I. Summary of runs.

Run number	Type of run	Cylinder set	Length of run
3	PuBe neutron source	None	0:03
4	Cs 137 source	None	0:01
5	Co 60 source	None	0:01
11	Cf source	None	0:40
12	Cf source	None	< 7:48
14	Cf source	None	0:10
20	Cf source	None	0:07
21	Cf source	None	< 0:10
22	Cf source	None	0:02
23	Signal timing calibration	None	0:19
30	Background	None	0:02
31	Background	None	0:20
32	Background	None	8:16
At this point we adjusted online gates, pulse shape discriminators, and the voltages of detectors U0 and D0			
33	Co 60 source	None	
34	Cf source	None	2:16
35	Background	$\frac{1}{2}$ lead brick <sup>a</sup>	1:20
36	Background	$\frac{1}{2}$ lead brick <sup>a</sup>	0:23
b			
40	Background	Set L	8:57
41	Background	Set L No. 13	3:33
42	Data run	Set A Nos. 1,2,3	6:15
43	Data run	Set A	12:30
44	Data run	Set B	9:22
45	Data run	Set C	9:46
46	Data run	Set D	7:23
47	Data run	Set D	7:53
48	Data run	Set E	9:47
49	Data run	Set E	6:26
50	Cf source	None	2:57
51	Background	Set F	7:30
52	Background	Set G	4:06
53	Data run	Set H	4:03
54	Data run	Set I	4:02
55	Data run	Set K Nos. 9,10,12	4:01
56	Data run	Set K Nos. 9,10,11	4:30
57	Data run	Set K Nos. 9,10,12	4:00
58	Data run	Set K Nos. 9,10,11	4:25
59	Cf source	None	1:00
60	Background	Set M	4:01
61	Data run	Set J	8:44

<sup>a</sup>A 5.1 cm × 10.1 cm × 8.9 cm lead brick was placed between detectors U0 and D0.

<sup>b</sup>Run 40 followed run 36 directly. There were no runs labeled as run 37, run 38, or run 39.

- (4) The cylinder was checked for leaks.
- (5) The cylinder was evacuated to  $< 10^{-4}$  Torr.
- (6) The cylinder was heated to 200°C for 1–2 hours.
- (7) The cylinder was cooled to room temperature.
- (8) The cylinder was valved off from the vacuum system, which was then flushed with D<sub>2</sub> gas several times at the end of which the vacuum pumps were valved off.
- (9) The cylinder was pressurized and valved off.

The vacuum system consisted of a liquid-nitrogen trapped glass vacuum rack and a Welch mechanical pump.

The first three cylinders were used over 8 cooling cycles, cylinder 4 was used over 10 cooling cycles, cylinders 6 and 8 over 3 cooling cycles, and the remainder of the cylinders (set K and cylinder 5, containing new samples not used in Ref. 2) were used for 2–4 cooling cycles. All neutron activities reported in the Los Alamos–BYU experiment (see Table III of Ref. 2) started during or before cycle 5, with some 12 bursts occurring during cycles 1–4 and none of the 21 reported bursts<sup>2</sup> beyond cycle 9. We therefore limited the major part of our experimental study to 8–10 cycles per cylinder. In addition, since in Ref. 2 it is reported that the majority of the bursts occur within an hour after the sample is allowed to warm up, the cycle duration in our experiment was shortened from the 24 hours or so used in Ref. 2, to 4–9 hours, see Table I. While warming up it took two hours for our cylinders to reach 0°C as determined by monitoring the cell's pressure.

Before the Ti662 alloys used throughout most of the experiments were loaded into the pressure cells, they were cleaned according to the protocol developed at Los Alamos<sup>2</sup> (see above). This was done to ensure that our samples were as close as possible in composition to those investigated in Ref. 2. Since the oxide layer on the alloys is not removed in this treatment,<sup>6</sup> it is highly unlikely that a significant amount of deuterium is incorporated into the metal lattice in these samples either through deuterization or chemisorption. The material from cylinder 1 was found to have a deuterium to titanium atomic ratio of  $1.3 \pm 0.1\%$  after the experiment.<sup>7</sup> The sample in cylinder 5 (set E), which contained used Ti-Pd alloy electrodes, fused Ti, and Pd was treated to remove the oxide layer. Thus it did have a significant amount of deuterium incorporated in the solid as was evident from both the heat produced and an immediate drop in the cylinder pressure, see Table II. This sample was used in two cooling cycles, and when no neutron activity was observed, new samples were prepared. In addition four cylinders prepared in Brookhaven National Laboratory were used as described in Table II, set K.

In a recent collaboration of five universities at Paris,<sup>8</sup> the Ti electrodes in the experiment reported in Ref. 1 were studied. It is reported<sup>8</sup> that the deposition of material from the complicated electrolyte used in Ref. 1 prohibited the insertion of deuterium into the lattice. The conclusion of Ref. 8 with respect to the original BYU experiment appears to be very similar to our con-

TABLE II. Cylinder sets used in experiments.

Cylinder set	Cylinder No.	Type of gas	Type of metal
Set A	No. 1	D <sub>2</sub> at 53 atm	60 g of thick Ti662 <sup>a</sup> chips <sup>2</sup>
	No. 2	D <sub>2</sub> at 67 atm	66 g of thin Ti662 chips <sup>2</sup>
	No. 3	D <sub>2</sub> at 46 atm	67 g of Ti662 chips <sup>c</sup>
	No. 4 <sup>b</sup>	D <sub>2</sub> at 17 atm	12 g of thin Ti662 chips <sup>2</sup> and 4g of Ti662 chips <sup>c</sup>
Set B	No. 1	D <sub>2</sub> at 49 atm	60 g of thick Ti662 chips <sup>2</sup>
	No. 2	D <sub>2</sub> at 67 atm	66 g of thin Ti662 chips <sup>2</sup>
	No. 3	D <sub>2</sub> at 46 atm	67 g of Ti662 chips <sup>c</sup>
	No. 4 <sup>b</sup>	D <sub>2</sub> at unknown atm	12 g of thin Ti662 chips <sup>2</sup> and 4 g of Ti662 chips <sup>c</sup>
Set C	No. 1	D <sub>2</sub> at 46 atm	60 g of thick Ti662 chips <sup>2</sup>
	No. 2	D <sub>2</sub> at 67 atm	66 g of thin Ti662 chips <sup>2</sup>
	No. 3	D <sub>2</sub> at 46 atm	67 g of Ti662 chips <sup>c</sup>
	No. 4 <sup>b</sup>	D <sub>2</sub> at unknown atm	12 g of thin Ti662 chips <sup>2</sup> and 4 g of Ti662 chips <sup>c</sup>
Set D	No. 1	D <sub>2</sub> at 45 atm	60 g of thick Ti662 chips <sup>2</sup>
	No. 2	D <sub>2</sub> at 67 atm	66 g of thin Ti662 chips <sup>2</sup>
	No. 3	D <sub>2</sub> at 46 atm	67 g of Ti662 chips <sup>c</sup>
	No. 4 <sup>b</sup>	D <sub>2</sub> at unknown atm	12 g of thin Ti662 chips <sup>2</sup> and 4 g of Ti662 chips <sup>c</sup>
Set E	No. 2	D <sub>2</sub> at 67 atm	66 g of thin Ti662 chips <sup>2</sup>
	No. 3	D <sub>2</sub> at 46 atm	67 g of Ti662 chips <sup>c</sup>
	No. 4 <sup>b</sup>	D <sub>2</sub> at unknown atm	12 g of thin Ti662 chips <sup>2</sup> and 4 g of Ti662 chips <sup>c</sup>
	No. 5	Comment d	
Set F	No. 6	H <sub>2</sub> at 54 atm	65 g of Ti662 chips <sup>2</sup>
	No. 7	D <sub>2</sub> at 54 atm	No chips
	No. 8	Vacuum	65 g of Ti662 chips <sup>2</sup>

TABLE II. (Continued).

Cylinder set	Cylinder No.	Type of gas	Type of metal
Set G	No. 6	H <sub>2</sub> at 50 atm	65 g of Ti662 chips <sup>2</sup>
	No. 7	D <sub>2</sub> at 53 atm	No chips
	No. 8	Vacuum	65 g of Ti662 chips <sup>2</sup>
Set H	No. 4 <sup>b</sup>	D <sub>2</sub> at unknown atm	12 g of thin Ti662 chips <sup>2</sup> and 4 g of Ti662 chips <sup>c</sup>
	No. 6	D <sub>2</sub> at 59 atm	65 g of Ti662 chips <sup>2</sup>
	No. 8	D <sub>2</sub> at 59 atm	65 g of Ti662 chips <sup>2</sup>
Set I	No. 4 <sup>b</sup>	D <sub>2</sub> at unknown atm	12 g of thin Ti662 chips <sup>2</sup> and 4 g of Ti662 chips <sup>c</sup>
	No. 6	D <sub>2</sub> at 58 atm	65 g of Ti662 chips <sup>2</sup>
	No. 8	D <sub>2</sub> at 58 atm	65 g of Ti662 chips <sup>2</sup>
Set J	No. 4 <sup>b</sup>	D <sub>2</sub> at unknown atm	12 g of thin Ti662 chips <sup>2</sup> and 4 g of Ti662 chips <sup>c</sup>
	No. 6	D <sub>2</sub> at 59 atm	65 g of Ti662 chips <sup>2</sup>
	No. 8	D <sub>2</sub> at 59 atm	65 g of Ti662 chips <sup>2</sup>
Set K	No. 9	D <sub>2</sub> at 27.2 atm	50 g of FeTi
	No. 10	D <sub>2</sub> at 28.2 atm	45.9 g of V(D <sub>2</sub> )
	No. 11	D <sub>2</sub> at 28.2 atm	20.3014 g of Y metal
	No. 12	D <sub>2</sub> at 13.6 atm	24.98 g of La(D <sub>3</sub> )
Set L	No. 13	H <sub>2</sub> at 53 atm	Empty
	No. 14	Vacuum	Empty
	No. 15	Vacuum	Empty
	No. 16	Vacuum	Empty
Set M	No. 17	Vacuum	50 g of FeTi

<sup>a</sup>Ti662 is an alloy of Titanium containing 6% Al, 6% V, and 2% Sn.

<sup>b</sup>This cylinder was smaller than the others and lacked a pressure gauge.

<sup>c</sup>Material from Ormet Corporation.

<sup>d</sup>This cylinder contained 36 g of Ti(80%)-Pd(20%) from powders sintered together, 21.0 g of Ti(90%)-Pd(105%) from powders sintered together, 25.7 g of Ti-Pd-V from powders sintered together, 7.8 g of fused Ti, and 5.0 g of Pd. These materials were used as electrodes in previous experiments on "cold fusion" in electrochemical cells. Upon exposure to an initial 6.8 atm of D<sub>2</sub> gas, these electrodes immediately underwent a hydriding reaction as evidenced by a sharp rise in the temperature of the pressure cell. The reaction had gone to completion before counting and no additional D<sub>2</sub> gas was added.

clusions with respect to the experiment of the Los Alamos-BYU collaboration.

The background was studied under several different conditions over several different experiments, see Table I (note that background Run 40 is the longest and thus has the greatest effect on the weighted background average in Fig. 6). The background experiments were carried out with no cylinders in the detector system (Runs 30-32), with a lead brick in place of the cylinders (Runs 35, 36), with evacuated cylinders without Ti chips (Runs 40, 41), with a cylinder including only Ti chips under vacuum (Run 51), with cylinders including Ti chips in hydrogen gas cooled to 77 K in liquid nitrogen (Runs 51, 52), and with a cylinder containing deuterium gas with no Ti chips (Runs 51, 52). The cell with just deuterium gas was used to study the possibility of neutrons arising from the photodisintegration of deuterium.

### B. Neutron detector

The experimental setup is similar to, but more efficient than, the one used in the previous Yale-Brookhaven colla-

boration<sup>5</sup> on "cold fusion." The reader is referred to Ref. 5 for details of the neutron detectors and veto counters as well as the operation of the detector system and the various cuts that can be placed on the pulse shape, pulse height, and time-of-flight (TOF) parameters in the analysis of the data. In Fig. 1 we show the experimental arrangement drawn to scale, with the two central detectors, U0 and D0, placed 2 cm from the cells and used as scatterers, and the ten ring detectors placed 17 cm from the cells.<sup>5</sup>

We list here the various improvements in the system as compared to that used in Ref. 5. Twelve neutron detectors were used in this experiment instead of the six used in Ref. 5. The detectors were arranged in two hemispheres allowing for measurement of up-down asymmetry. In this way we discriminate, in the upper hemisphere, between downward moving (background) neutrons and upward moving neutrons expected to have originated in the cells, see below. In addition, the two central detectors are placed closer to the cell's position, see Fig. 1, and have a larger efficiency for events occurring in the cell's position, further enabling us to discriminate

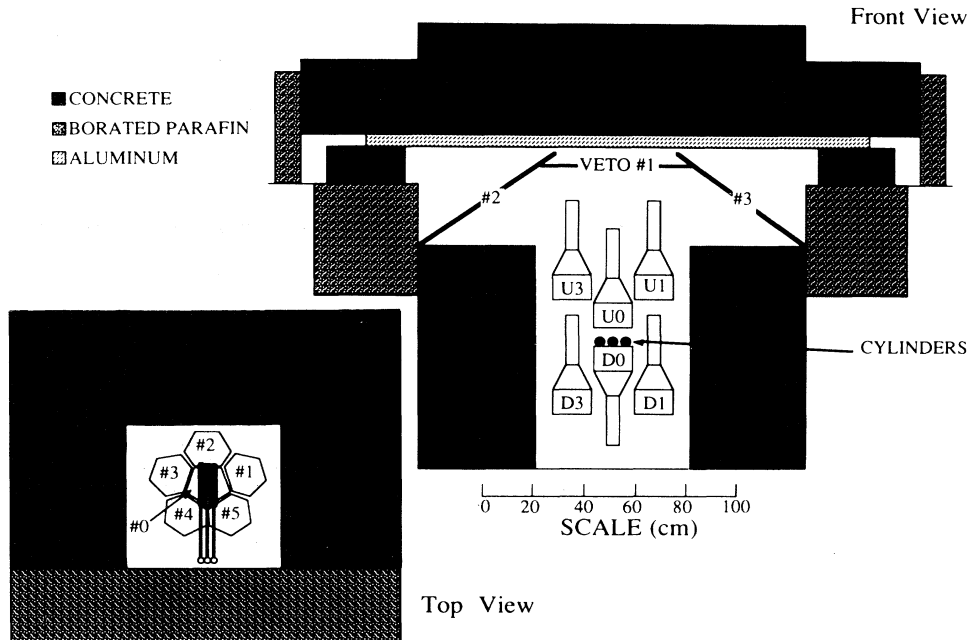


FIG. 1. A schematic diagram of the experimental arrangement drawn to scale.

against background events as we demonstrate below. Three veto counters were used to span a larger solid angle than the two used in Ref. 5. The shielding of the setup was much improved, with the use of some 20 tons of concrete blocks containing iron (of dimension  $45 \times 45 \times 60$  cm, each).

### C. Detector efficiency

The total efficiencies (intrinsic efficiency times solid angle efficiency) of our neutron detectors were measured using a  $^{252}\text{Cf}$  source placed in the center of the detector system and on the edge of the pentagonal central detectors. We refer the reader to Ref. 5 for the discussion of the energy spectrum of neutrons from the  $^{252}\text{Cf}$  source and details of the method for measuring the detector's efficiency using this source. The efficiency of the central detectors was found to be  $\epsilon(\text{U0}) = \epsilon(\text{D0}) = 10 \pm 3\%$ , and the efficiency of each detector in the outer rings, U1–U5 and D1–D5, was measured to be in the range of 0.5–1.1%. We have used the average value of 0.8% for the efficiency of ring detectors in the calculations described below. Thus, when all detectors are used without requiring time-of-flight coincidences ("singles mode"), a total efficiency of  $28 \pm 5\%$  is obtained. The time of flight coincidence efficiency between the central detectors, U0 or D0, and one of their respective ring detectors— $U_i$  or  $D_i$  ( $i = 1, \dots, 5$ ), was measured to be  $0.2 \pm 0.1\%$ , yielding a total coincidence efficiency of  $2 \pm 1\%$ .

### D. Discrimination Against Background

The efficiency of the central detectors is a factor of 12 larger than that of each of the ring detectors. For a neutron burst of multiplicity  $M$ , the probability that

one and only one central detector ( $\epsilon = 0.1$ ) and at least one out of ten ring detectors (total  $\epsilon = 0.08$ ) fires is  $2(1 - 0.9^M)0.9^M(1 - 0.92^M)$ . The probability that neither central detector fires and one ring detector fires is  $0.8^M(1 - 0.92^M)$ . For a multiplicity  $M \geq 50$  ( $M \geq 100$ ) the probability that a ring counter fires without both central detectors firing is at the most 1% (0.005%). For background events not related to the neutrons generated through interaction of cosmic rays with the cylinders, the efficiency of all detectors is essentially the same, allowing a situation where the ring counters fire with one of the two central detectors not firing. The requirement that the two central detectors fire in a burst (of at least 50 neutrons) is very useful for discriminating against background cosmic neutrons.

The probability for a neutron double hit in one ring detector is given by (a binomial distribution)

$$P_D = \binom{M}{2} \epsilon^2 (1 - \epsilon)^{M-2} \quad (1)$$

with  $\epsilon = 0.8\%$ , and for a burst of as many as  $M = 50$  (100) neutrons originating at the cell's location, the double hit probability for a ring detector is only  $P_D = 5\%$  (15%). The fusion of  $^2\text{H} + ^2\text{H} \rightarrow ^3\text{He} + n$  yields 2.45 MeV neutrons which deposit their energy in our detector by scattering off protons in the liquid scintillator. The response of our detector<sup>5</sup> is such that the energy deposited in the detector varies from zero to the neutron energy with equal likelihood. Hence, the probability of observing a pulse height in excess of 2.45 MeV in our detector (i.e.,  $E > 2.45$  MeV where  $E$  is the energy deposited in our detector), as a consequence of a double hit from two neutrons of 2.45 MeV each, is given by

$$P_D(E) = \int_{x_0}^{\infty} F(x) dx \int_{1-x}^{\infty} F(y) dy, \quad (2)$$

where  $x_0 = E_{\min}/2.45$ ,  $E_{\min} = E - 2.45$ , the minimum energy deposited by each neutron, and  $F(x)$  is the detector's response function, including its pulse height deficiencies and finite resolution. It should be noted that due to pulse-height deficiencies in liquid scintillator the light produced by two recoiling protons, of for example 1 and 2.5 MeV, is summed to yield the light output corresponding to that of a proton of only 3.0 MeV recoil energy. For example, for a double hit summing up to 3.5 MeV in a ring detector, we find  $P_D(E=3.5)=37\%$  and for a double hit summing to 4.4 MeV we obtain  $P_D(E=4.4)=21\%$ . Furthermore, in order that the energy deposited by two neutrons in our detector be fully summed, the two neutrons must hit the detector within the rise time of the detector. The rise time of our neutron detectors is 5 nsec, and a 2.45 MeV neutron takes approximately 5 nsec to travel across the width (10 cm) of the detector. The fast rise time of our detector then leads to an additional correction factor, of at least 0.63, for the double hit probability. The double hit efficiency is then given by  $\epsilon_D \leq 0.63 P_D P_D(E)$ , and we conclude that the observation of a pulse height larger than 3.5 MeV in a ring detector can arise from a double hit with a very low probability of at most 4% for all possible multiplicities discussed below. For a double hit summed to 4.4 MeV in a ring detector (see below) this probability amounts to less than 2%. We conclude that the knowledge of the energy deposited in the ring detectors is crucial for discriminating against background neutron events.

The efficiency for vetoing cosmic-ray related events was measured, as described in Ref. 5, to be of the order of 65% for events occurring in the central detector. In addition, we estimated, from our  $^{252}\text{Cf}$  source data, that the efficiency for detecting 2.45 MeV neutrons in the veto counters is 0.6%. This source also yields gamma rays which make the measurement of neutron efficiency of the veto counters very hard as the plastic scintillator veto counters do not allow for neutron to gamma discrimination. Using known scattering lengths of neutrons in plastic scintillator material we calculate the self veto efficiency, with the threshold set at neutron energy of 2 MeV (0.7 MeV electron equivalent), to be approximately 0.35%. Thus for a burst of 50 (100) neutrons the self veto efficiency is estimated to be of the order 26% (45%). Therefore, we do not use the veto condition to exclude any data and such events were still analyzed in detail.

For each detector we measured its pulse shape (to facilitate neutron to gamma discrimination), its pulse height (for discrimination against background events, see above), and the time of flight between a start pulse from the central detector and a stop pulse from a ring detector.<sup>5</sup> The time-of-flight information allows the study of the time ordering of events and the discrimination against downward moving background neutrons. For background neutrons moving downward in the upper hemisphere a ring counter will fire before U(0) which creates a negative time of flight. For neutrons originating at the cell's location we have positive time of flight. This leads to a lower background rate, only 0.4 cph, in the upper hemisphere.

### E. Gate length

An event was accepted only when a signal was registered in one of the two central detectors, U0 or D0. A 20  $\mu\text{sec}$  wide gate generated from a hit in either one of the two central detectors was used for accepting all data falling within  $\pm 10 \mu\text{sec}$  of the trigger (i.e., within 10  $\mu\text{sec}$  before or after one of the two central detectors fired). For two successive hits separated by 10  $\mu\text{sec}$  in the two central detectors (or two successive hits in one central detector) the gate duration would then be further extended by an additional 10  $\mu\text{sec}$ . For example, for a burst of 130 (150) neutrons uniformly spread over 100  $\mu\text{sec}$  (the gate duration of Ref. 2) there is a 94.5% (96.5%) chance of detecting one neutron in either one of the two central detectors out of the 13 (15) neutrons during each period of 10  $\mu\text{sec}$ . The successive detection of neutrons would extend the gate duration. For the above example there is a 48% (50%) chance of having 13 (19) successive hits, each within 10  $\mu\text{sec}$  of the previous hit, in either one of the two central detectors. On the average these successive hits will be separated by 5  $\mu\text{sec}$ . Thus the gate duration would be 20  $\mu\text{sec}$  for the initial hit with an additional 5  $\mu\text{sec}$  added, on average, for each successive hit. This will then yield a gate duration of 80 (110)  $\mu\text{sec}$  during which all pulses will be accepted by our computer. Only at the end of the gate period will our peak searching ADC's start the conversion of analog signals to digital information.

For the time-of-flight data we used Nuclear Data NIM ADC's (ND581) with conversion dead time of 5  $\mu\text{sec}$ ; for the pulse height data we used Ortec CAMAC ADC's (AD811) with conversion dead time of 80  $\mu\text{sec}$ , and for the pulse shape data we used Lecroy CAMAC TDC's (LC2228) with conversion dead time of 100  $\mu\text{sec}$ . The ten Nuclear Data NIM ADC's, which read the time-of-flight data from the separate TAC's, were interfaced to our CAMAC crate via a fast readout MUX module produced at Argonne National Laboratory, see Appendix D, part (3). The setup is such that two simultaneous hits in the two central detectors arrive at the computer within 50 nsec of each other, and in the singles mode the gating is such that no data from any detector is lost over the gate duration.

In the coincidence time-of-flight mode the range of the TAC's was set to 10  $\mu\text{sec}$  over 8192 channels,<sup>5</sup> allowing for the study (in the coincidence mode only) of the time structure of bursts spanning 10  $\mu\text{sec}$  with a precision of 1.25 nsec. The time resolution of the system was measured for  $\gamma$ - $\gamma'$  events to be 2.5 nsec as discussed in Ref. 5. The detectors were calibrated using standard radioactive sources<sup>5</sup> and the knowledge of the response of the detector to various radiations as discussed in Ref. 5. The data were taken at the A. W. Wright Nuclear Structure Laboratory at Yale University over a ten day period and were written onto magnetic tapes event by event for analysis using the various cuts discussed in Ref. 5.

## III. EXPERIMENTAL RESULTS

In Fig. 2 we show a typical two-dimensional surface plot of pulse height versus pulse shape for  $^{252}\text{Cf}$  source

data exhibiting good gamma to neutron separation. This separation is obtained even at the low threshold used in this experiment, 50–70 keV electron equivalent (200–280 keV proton recoil energy, hence neutron energy loss).

#### A. First-level analysis

In this analysis a very broad gate is chosen on the pulse shape data (in one dimension) as shown in Fig. 2. This

broad gate makes certain that no neutrons are excluded, while at the same time including a considerable number of background gamma rays (and background neutrons), see below. For the background runs more than 90% of the pulse shape signals which survive the gate are gamma rays. In Figs. 3(a) and 3(b) we show a histogram of the number of detectors fired (event fold) using the liberal gate on the neutron pulse shape shown in Fig. 2. In this analysis multiple successive hits of neutrons in one detec-

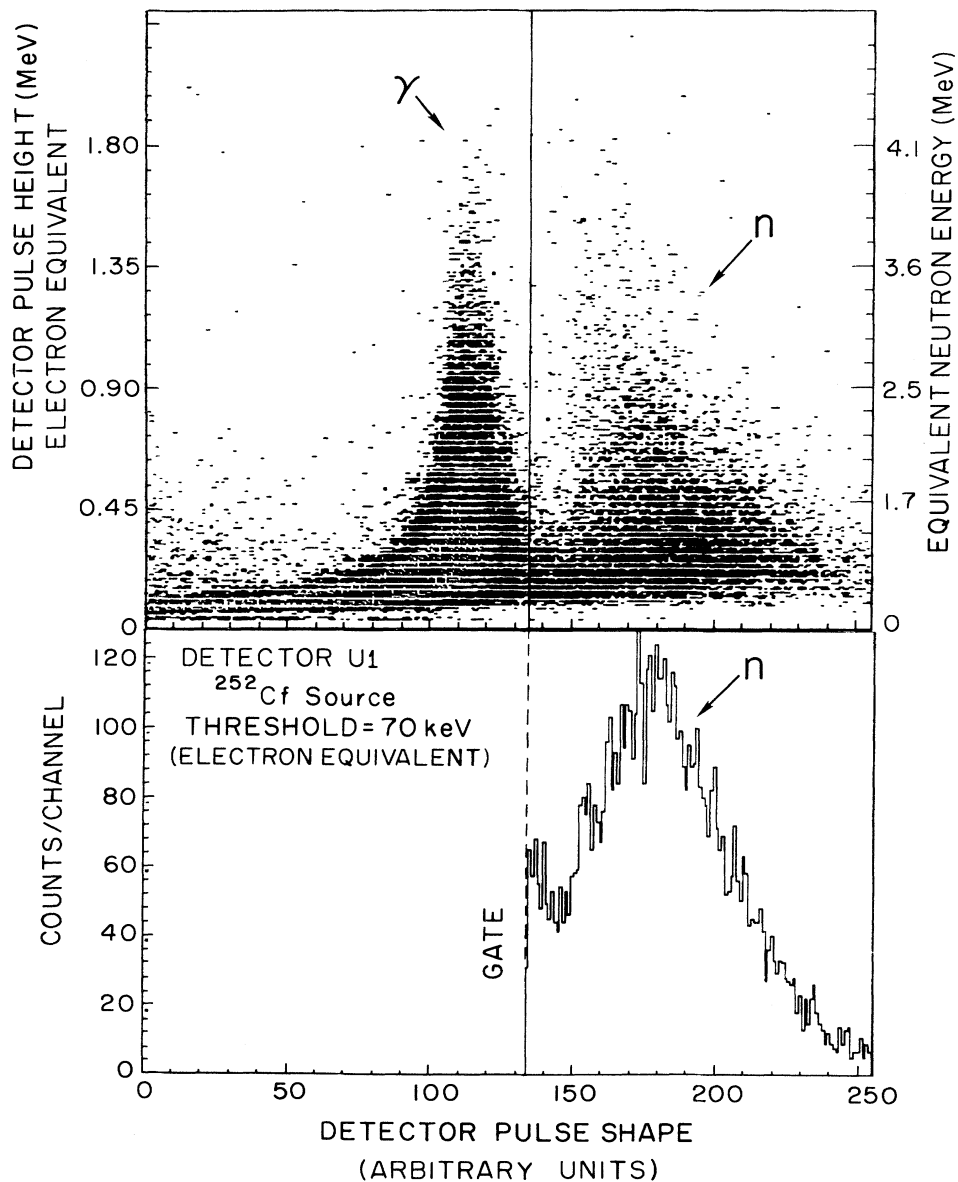


FIG. 2. Typical two-dimensional pulse height vs pulse shape plot for neutron detector U1. In a first-level (more liberal) analysis the very broad one-dimensional gate was used, as shown in the projection along the pulse shape axis. Events listed in Table III as neutron or gamma events have pulse shapes that fall within 10 channels of the gate's limit (around channel 140). Note the good neutron to gamma separation even at this low threshold.

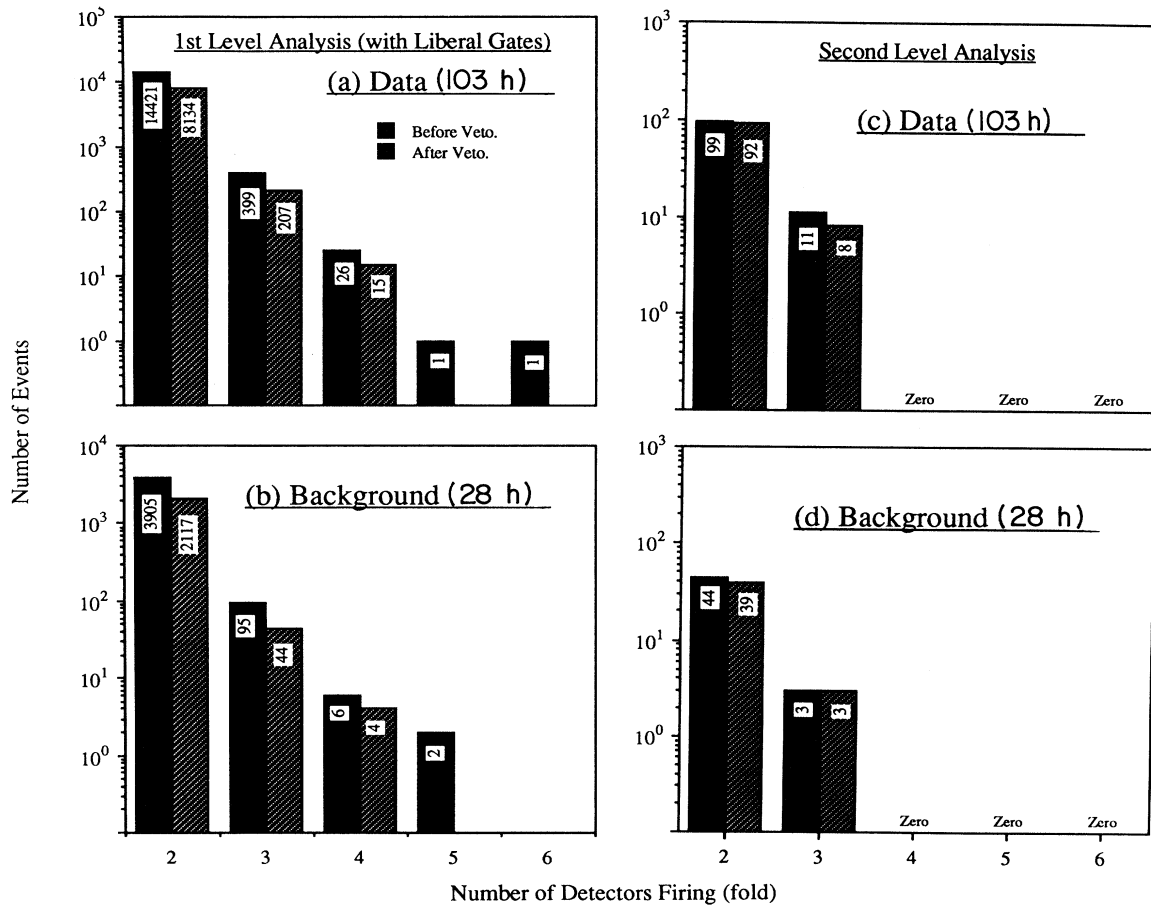


FIG. 3. Total number of detectors fired (fold): (a) and (c) for data runs and (b) and (d) for background runs, with or without a veto condition from the cosmic-ray detector. In (a) and (b) we show the fold pattern obtained from the first-level analysis (using the liberal gate shown in Fig. 2), and in (c) and (d) we show the results of the second-level analysis, as discussed in the text. All four high-fold events, shown in (a) and (b), are vetoed.

tor within our gate are counted as a fold  $K=1$  event. Only four events were observed to have high-folds in the whole array (including hits in both central and ring detectors) of  $K=5$  or 6. Two were observed in separate background runs (runs 40 and 51) and two were observed in separate data runs (runs 45 and 61). All four high-fold events were vetoed by the cosmic ray counter as shown in Fig. 3.

### B. Second-level analysis

In this analysis we placed cuts on the two-dimensional spectra shown in Fig. 2. In addition we required that *both* U0 and DO fire (see above) and applied a cut on pulse height to exclude events for which more than 3.5 MeV energy is deposited in a ring counter (see above). Note that the probability for a chance coincidence between a cosmic neutron (rate = 100 cph) and a neutron from a burst is of the order  $10^{-6}$  for a gate width of 20  $\mu\text{sec}$ , justifying exclusion of an event in which one of the

ring counters registers a pulse height larger than 3.5 MeV. Using this analysis, no events of total fold  $K > 3$  are observed (i.e., no more than one ring detector fired) in any of the runs, see Figs. 3(c) and 3(d).

In Fig. 4 we show the time distribution of the four high-fold events, as obtained with the first-level analysis using the less restrictive one-dimensional gate on the pulse shape. The time calibration is 0.9 min per channel, and  $t=0$  is a few minutes into the warmup cycle. Note that in the data shown in Figs. 3 and 4 we also observe the same rate, within uncertainties, for folds  $K=4$  and lower, as in the background runs. Indeed, no statistically significant deviations from the background were observed for low-fold events in any of the runs.

The list of observed event parameters for the four high-fold events of the first-level analysis is given in Table III. Three out of four of these events have pulse shapes which are on the border of our (one dimensional) pulse shape gate and are accepted here only due to our wide gate. In only one event (during run 45) did we observe

only pulse shapes expected for neutrons, and only in this event did both central detectors U0 and D0 fire. As shown above, the probability for a burst of at least 50 neutrons from fusion during which one of the central detectors D0 or U0 does not fire is less than 1%. As can be seen in Fig. 4, the event of run 45 occurred one hour and twenty-one minutes into warmup cycle 4 for cylinders 1–3 (cycle 3 for cylinder 4) at a temperature of approximately  $-10^\circ\text{C}$  as deduced from the cell's pressure. In this event, detector U5 registers at least 4.4 MeV, but the probability of observing 4.4 MeV in a ring detector was shown to be less than 2%, and we conclude that this event most likely arises from cosmic neutrons. As can be seen in Table III, in all four of these high-fold events the energy deposited in at least one ring detector is of the order of 4.4 MeV, in excess of the 2.45 MeV expected from a fusion event. We thus conclude (with at least 90% confidence) that all high-fold events are consistent with background events. It is worth noting that the detectors (D5 and U5) that register a large energy deposit from cosmic neutrons are located nearer to the less shielded front side of the setup which has only paraffin shielding without concrete, see Fig. 1.

Inspecting the time scale and energy deposited in detectors U5, U1, and U0 in the event of run 45 listed in

Table III, we may suggest that the event is consistent with a high-energy ( $E > 7.3$  MeV) cosmic-neutron (arriving from the less shielded front side, see Fig. 1) that undergoes triple scattering. It starts with one large angle scattering from detector U5 to its immediate neighbor, detector U1, depositing a large energy (4.4 MeV) in detector U5. The neutron then travels its mean free path in liquid scintillator (a few cm) in about one nsec and undergoes a small angle scattering in detector U1 towards the central detector U0. From U1 it travels for 17 nsec to the central detector U0. This time period is listed in Table III as negative, since in this case the ring counter was hit before the central detector, as would be expected for a downward moving cosmic neutron. Note that a neutron with a kinetic energy of approximately 2 MeV travels, on average, for some 15 nsec between a ring detector and a central detector. It appears that the parameters of the high-fold event of run 45 listed in Table III, can be explained by this hypothesis of one high-energy neutron executing triple scattering between detectors U5, U1, and U0.

### C. Upper limits

We have calculated the fold probability in our array using the formalism first developed by B. R. Mottelson as

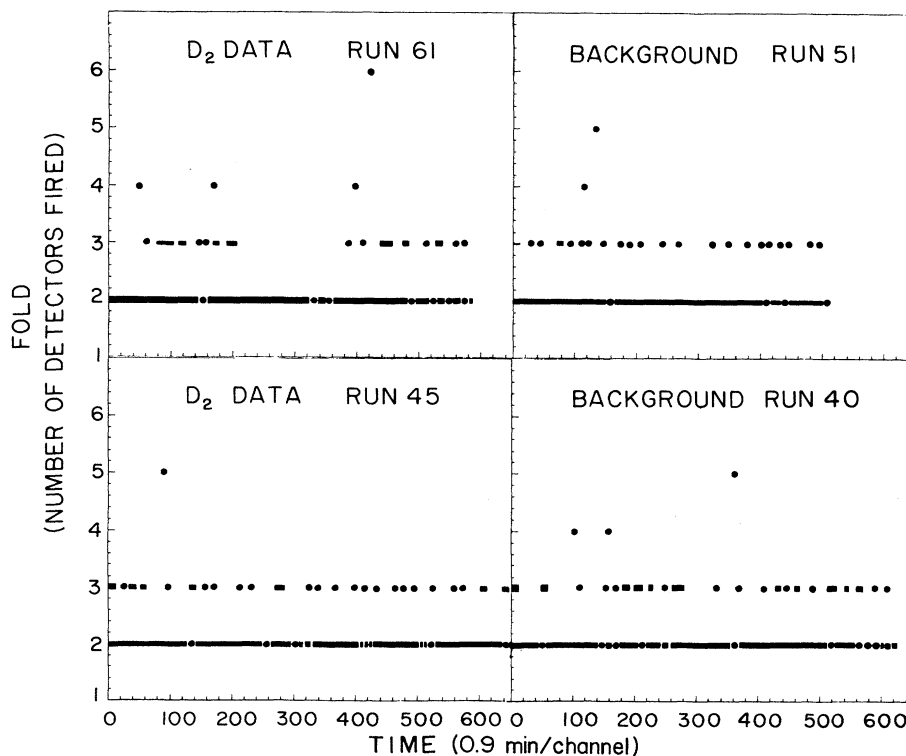


FIG. 4. Total event fold (in the entire array), as a function of time into the warmup cycle, using the liberal gates of the first-level analysis. The time calibration is 0.9 min per channel, and  $t=0$  is a few minutes after the cylinders were removed from the liquid-nitrogen bath.

TABLE III. Summary of high-fold events.

Detector	Energy deposited (MeV)	Time of flight (nsec)	Pulse shape
Fivefold event in background run 40			
U0	2.8	0.0	<i>n</i>
U2	0.9	3.7	<i>n</i>
U4	0.9	3.7	<i>n</i> or $\gamma$
U5	4.4	-2.4	<i>n</i> or $\gamma$
D2	1.5	N/A	<i>n</i>
Fivefold event in background run 51			
U3	0.4	N/A	<i>n</i> or $\gamma$
U4	2	N/A	<i>n</i>
U5	4.4	N/A	<i>n</i> or $\gamma$
D0	0.9	0.0	<i>n</i> or $\gamma$
D1	1.5	3.7	<i>n</i> or $\gamma$
Fivefold event in data run 45			
U0	1.8	0.0	<i>n</i>
U1	1.1	-17	<i>n</i>
U3	0.6	3800	<i>n</i>
U5	4.4	-18	<i>n</i>
D0	3.3	N/A	<i>n</i>
Sixfold event in data run 61			
U1	0.6	N/A	<i>n</i>
U4	0.4	N/A	<i>n</i>
D0	5.4	0.0	<i>n</i> or $\gamma$
D2	1.6	740	<i>n</i> or $\gamma$
D4	1.1	1.2	<i>n</i> or $\gamma$
D5	4.2	1000	<i>n</i>

reviewed in Refs. 9–11. The fold probability in our array of twelve detectors is determined by the ten ring detectors; therefore, we only consider the fold probability in the ring counters. For an array of ten (ring) detectors the

fold probability,  $P_K(M)$ , of observing  $K$  ring detectors fired ( $K$ -fold event), for a neutron burst of Multiplicity  $M$  is given by

$$P_K(M) = (-)^{10+K} \binom{10}{K} \sum_{i=1}^{10} (-)^{i+1} \binom{K}{10-i} [1 - (1-i\varepsilon)^M], \quad (3)$$

where  $\binom{N}{I}$  is the usual binomial coefficient (equal to zero for  $I > N$ ), and  $\varepsilon = 0.8\%$  is the efficiency of a single ring detector. Note that Eq. (14) of Ref. 9 is missing the binomial coefficient  $\binom{10}{K}$ , which however is correctly inserted in Eq. (15) of Ref. 11. Detailed Monte Carlo simulations<sup>12</sup> confirm the validity of Eq. (3).

The total efficiency of the ten ring detectors is given by  $1 - \varepsilon'$ , where  $\varepsilon' = (1 - 10\varepsilon)^M$  is the inefficiency of the array. Note that the array's inefficiency is given by a fold  $K = 0$  event (i.e.,  $\varepsilon' = P_{K=0}$ ). For example, for a multiplicity of 25 (35) the total efficiency of our counters is 88% (95%). We note that for a given event the sum of all fold probabilities for folds  $K = 1, \dots, 10$  must equal  $1 - \varepsilon'$ . This would be required since we either miss the detection of the event or observe a 1,2,3, etc. fold event, with an efficiency of  $1 - \varepsilon'$ , (i.e.,  $\sum_{K=0}^{10} P_K(M) = 1$ ).

In Fig. 5 we show the fold probability of our array calculated using Mottelson's exact solution,<sup>9</sup> Eq. (3). For an event of multiplicity  $M = 100$ , the array's total efficiency is 99.98%, and the most likely event is of fold  $K = 5$  or 6 (i.e., seven or eight neutrons detected in the entire array). No such events were observed in any of our experiments.

Since, for  $M = 100$ , we have at least 90% probability for observing a fold  $K = 4$  or larger event (i.e., 6 or more neutrons detected in the entire array), see Fig. 5, the first level analysis (using a very liberal gate) yields to an upper limit on the burst size of 100 with 90% confidence. As shown in the event parameters listed in Table III, this analysis is clearly allowing a large number of background

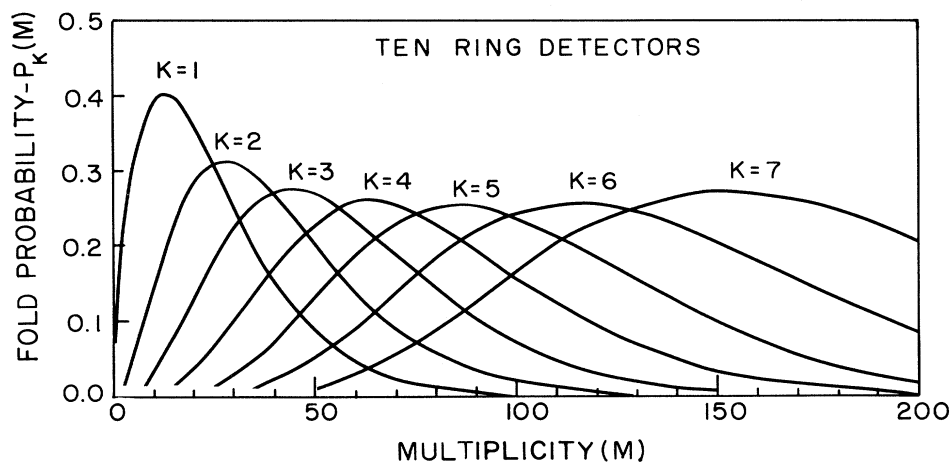


FIG. 5. The fold probability  $P_K(M)$ , for the ring detectors, calculated using Eq. (1).

events to be accepted. Having established a first-level analysis upper limit of 100, we use our previous estimates for double hits, etc. with  $M < 100$  (see Sec. II D), and we apply the cuts of the second-level analysis. As discussed in Sec. II D the probability of removing a true fusion neutron event through the use of our cuts is less than 5%. We estimate that for multiplicity  $M > 50$  we have at least a 90% probability of observing a  $K=2$  or larger fold event (i.e., four or more neutrons detected in the entire array). Since no valid events are observed of more than one fold in the ring detectors, in our second-level analysis, see Fig. 3(c), we deduce (with 90% confidence) an upper limit on the size of neutron bursts of 50.

Based on the early data of Menlove *et al.*,<sup>2</sup> we expect (see Appendix C) on the average as many as 4.8–12 neutron bursts of 70–300 neutrons over the duration of our experiment. As discussed in Appendix C we note that the burst rate reported in the early work of Menlove *et al.*<sup>2</sup> was much reduced in subsequent reports.<sup>3,4</sup> Parameters essential for the estimate of the burst rate such as the running time of the later Los Alamos-BYU experiments<sup>3,4,15,16</sup> and the gate duration are uncertain. Taking into account the worst possible scenario (see Appendix C), in the later data we only estimate, on the average, as little as 0.4 bursts to occur in our data. For  $N$  expected bursts, the probability that a burst will in fact occur in our experiment is  $1 - e^{-N}$ , see below. For an expected occurrence of two bursts in our experiment it is 86%. We then conclude that our data rules out with at least 90% confidence the evidence for “cold fusion” as reported in the early work of Menlove *et al.*<sup>2</sup> which leads to at

least four bursts expected in our data. In order to test the later results<sup>3,4</sup> one may need to run for as long as two months to rule out this later, lower rate.

In Fig. 6 we show the rate above background of neutrons emitted randomly. For these data the time-of-flight coincidence method was used<sup>5</sup> which yielded the very low background of 2 cph (0.4 cph in the upper hemisphere and 1.6 in the lower hemisphere). Using the backgrounds measured in runs 40, 41, 51, 52, and 60, we deduce the neutron rates above background shown in Fig. 6, which exhibit no significant deviation from the background. The ensemble average of all our data yields the rate  $-0.2 \pm 0.4$  cph above background. We then deduce (with 90% confidence) the random emission of neutrons not to exceed 0.6 cph, corresponding to a neutron source of 30 neutrons/hour (0.008  $n$ /sec). This upper limit is a factor of 6 to 25 smaller than the observed range of rates above background reported in Ref. 2.

#### IV. CONCLUSIONS

We have searched for the emission of neutron bursts from Ti samples (as similar as possible to the ones used by Menlove *et al.*) using an array of neutron detectors with high efficiency for the detection of several neutrons from a large burst. No statistically significant deviations from the background were observed, and we obtain upper limits on neutron emission, in both burst and random emission modes, which are significantly lower than the evidence for “cold fusion” reported by Menlove *et al.* in Ref. 2, i.e., during the early period.

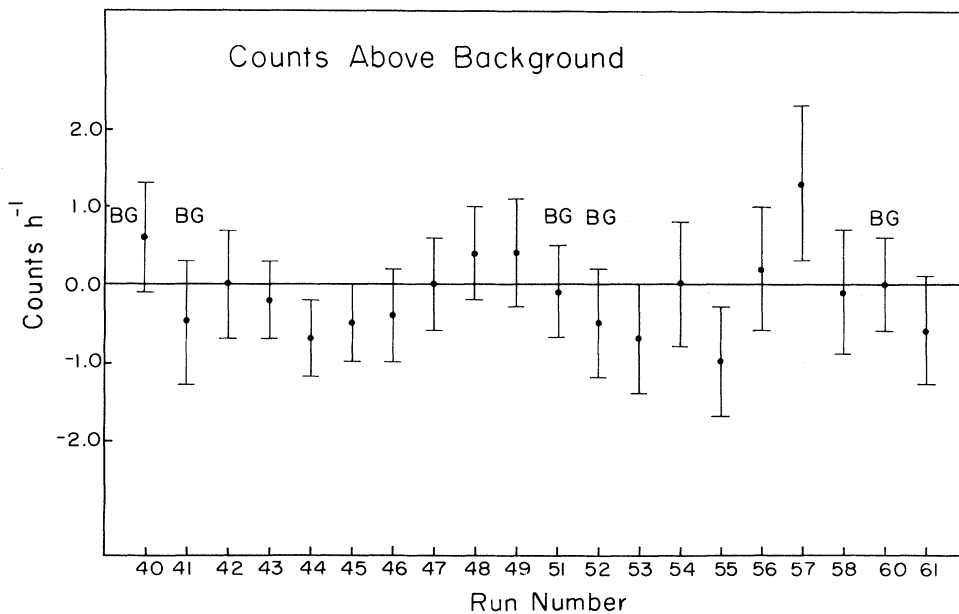


FIG. 6. Neutron count rates above background, for random emission. The ensemble average corresponds to the rate of  $-0.2 \pm 0.4$  cph above background. Runs 1–36, 50, and 59 are setup and calibration runs. Note that the length of the runs varied from 3.5 to 12.5 hours (see Table I); therefore, the apparent systematic structure is not meaningful.

### ACKNOWLEDGMENTS

We thank S. E. Jones for providing the Ti alloy samples, cylinders, and detailed preparation procedures of the samples, as used in the Los Alamos–BYU collaboration. We thank S. E. Jones and A. Anderson for separately analyzing the data and pointing out some of the systematics discussed in Appendix D. In our previous report of the Yale-BYU-BNL collaboration,<sup>13</sup> only the approximation Eq. (7), see below, was used due to an oversight. We thank S. E. Jones for useful comments concerning this research. We thank R. L. Garwin for offering his intriguing solution for fold probability as outlined in our Appendix A. We also thank R. L. Garwin for several illuminating discussions and bringing to our attention Ref. 3 of the Los Alamos–BYU collaboration. We thank J. E. Hack and K. W. Zilm of Yale University and J. Reilly of Brookhaven National Laboratory for help in preparing our samples, and we thank J. R. Beene for useful conversations. This work was supported in part by U.S. Department of Energy Contract No. DE-AC02-76ER03074.

### APPENDIX A: FOLD PROBABILITY

In deriving Eq. (3) standard calculations of fold probabilities are used.<sup>9–11</sup> In the following we outline a somewhat different and more elegant solution provided to us by R. L. Garwin. We emphasize, however, that the two solutions agree within a few percent.

For an array of  $N$  detectors of efficiency  $\epsilon$  each and a neutron burst of  $M$  neutrons, the expected average number of hits in a counter is  $M\epsilon$ . The striking of a detector by neutrons is a Bernoulli (binary) process with  $M$  trials with a success chance of  $\epsilon$  each. The consequence of this process is a certain number of hits ( $I$ ) in a detector with a probability given by the binomial distribution:<sup>14</sup>

$$P(M, \epsilon; I) = \binom{M}{I} \epsilon^I (1 - \epsilon)^{M-I}. \quad (4)$$

In the limit of small value of  $\epsilon$ , this probability behaves like the Poisson distribution:<sup>14</sup>

$$P(\mu, K) = e^{-\mu} \mu^K / K! \quad (5)$$

with the mean hit number in a detector of  $\mu = \epsilon M$ . For example, for  $M = 50$  we find a double hit probability ( $I = 2$ ) of 5%, as deduced previously from Eq. (1). Therefore the probability that no hits occur in a detector is  $e^{-M\epsilon}$ , and the probability that a detector is struck by neutron(s) is  $1 - e^{-M\epsilon}$ . If a detector has only one vote independent of the number of hits in it, only these two values are of significance. The probability that none of the  $N$  detectors in our array were struck (fold  $K = 0$ ) is then  $P_0 = (e^{-M\epsilon})^N$ , and the probability that precisely one (ring) detector fires (fold  $K = 1$ ) is given by  $N(1 - e^{-M\epsilon})/e^{-M\epsilon} P_0$ . The probability for a fold  $K$  event is then

$$P_K(M) = \binom{N}{K} (1 - e^{-M\epsilon})^K / e^{-M\epsilon} P_0. \quad (6)$$

Equation (6) is equivalent to our solution Eq. (3) and gives identical results to those shown in Fig. 5. Equation (6) is however more easily applied for a general array

(with detectors of different efficiencies) and yields a more transparent solution.

### APPENDIX B: AN APPROXIMATION FOR THE FOLD PROBABILITY

As discussed in Ref. 8, Eq. (3) could be approximated by

$$P_K(M) = M! 10\epsilon (M-1) 9\epsilon \cdots (M-K+1) (10-K+1) \epsilon / k!. \quad (7)$$

Care should be used in using the approximation, Eq. (7), as it is only valid for probabilities smaller than 50% (for large  $M$ , it is in fact larger than 1). We note that use of this approximation led us to conclude in a preliminary report<sup>13</sup> an upper limit on the burst size of 27. The upper limit deduced in this paper using the exact solution of Eq. (3) is 50.

### APPENDIX C: ESTIMATE OF EXPECTED NUMBER OF BURSTS

In order to estimate the number of bursts expected in our experiment a detailed description of the observed burst statistics, running time, down time, etc., of the Los Alamos–BYU experiment is needed. These data have not been made available in any of the published material of the Los Alamos–BYU collaboration. Thus, we have to rely on partial reports of these data<sup>2–4</sup> (which appear to be inconsistent on some data) and private communications from S. E. Jones and H. O. Menlove.

The Los Alamos–BYU collaboration reports two different burst rates. Early in their experiment H. O. Menlove reported at the International Workshop on Cold Fusion, held at Santa Fe, at least 12 bursts of 70–255 neutrons occurring over a period of 22 days with at least 6 of these bursts including approximately 120 neutrons or more. Note that we have rounded off the number of neutrons per burst in order to bin them in groups of ten. These data were also reported in the first version of Ref. 2 that covers the same time period. All twelve of these bursts were observed during warmup time; therefore, it is stated<sup>2–4</sup> that the warmup period is the crucial one for observing bursts. Hence, we only consider the warmup time in the following estimates of the burst rate. During this time period at least twelve bursts of 70–255 neutrons were observed over 22 days of data acquisition.

Experiments using four detection systems over four and a half months are described in Refs. 3 and 4. But in Refs. 3 and 4 we find only 20 bursts of 50 or more neutrons observed while the cylinders are warming up (ten such bursts observed at room temperature). Out of these 20 bursts, ten were in excess of 120 neutrons. While the earlier-reported burst rate is one burst per less than 2 days,<sup>2</sup> the later-reported rate<sup>3,4</sup> corresponds to approximately one burst per 7 days.

If we make the upper-limit assumption that the down time for the experiment was zero and that data were collected over all days (including weekends) with the use of

all four systems without interruption for background measurement, calibration, service of detectors, etc., we are led to the estimate of 2200 hours in the early period<sup>2</sup> and between 5700 and 13 000 hours used over the four and a half months.<sup>3,4</sup> We emphasize that in Ref. 2 we find that at least during part of the time, i.e., at the initial stages of the experiment, some systems were used for measurements of background. Hence, this time estimate of 2200 hours for the early period provides only an upper limit on the useful running time of the Los Alamos–BYU experiment. While it is stated<sup>15</sup> that running time of the later period corresponds to 13 000 hours running, we can only find published accounts<sup>3,4</sup> of experiments with 34 Ti samples. In our experiment seven samples which include Ti were used (see Table II). If we assume that each sample was run for one week then we calculate a lower limit of 5700 hours. However, since the exact durations of each of these experiments has not been made available to us,<sup>16</sup> the actual running time is only known to within a factor of 2.

In Ref. 3 it is reported that during only 5% of the running time were the cylinders at temperatures below 0°C, warming up from 77 K. In contrast, the warmup time is listed as only 2% of the total time in Ref. 4. We will use both figures in our estimates. We then estimate the useful running time at warmup temperatures to be at least ( $2200 \times 0.02 =$ ) 44 hours and at most ( $2200 \times 0.05 =$ ) 110 hours for the early period<sup>2</sup> and at least ( $5700 \times 0.02 =$ ) 114 hours and at most ( $13\,000 \times 0.05 =$ ) 650 hours for the later period.<sup>3,4</sup> Note that this running time estimate includes the assumption that all four systems were running concurrently and therefore does not correspond to “real time.”

In our experiment from a total of 88 hours of running with Ti662, approximately 20 hours (of “real time”) occurred during the warmup period (neglecting the running time with samples made at Brookhaven). On the average, four samples were used over 10 cycles each with 2 hours at temperatures below 0°C.

On the average, the Ti samples used in the Los Alamos–BYU collaboration contained 83.7 grams of Ti chips per cylinder (see Table II of Ref. 2) or 82.3 grams per cylinder (see Table II of Ref. 3 and an addition to it by S. E. Jones in a private communication). In our experiment we used on the average four cylinders containing a total mass of 184.4 grams of Ti chips.

While in the Los Alamos–BYU experiment approximately 30% of the neutrons in a burst are counted, in our data we would detect approximately 10% of the neutrons in a burst, see Fig. 5. Nevertheless, the efficiency for measuring neutrons from a burst in both experiments is in excess of 95%.

This leads to four estimates of the expected burst rate in our data. Based on the early reports<sup>2</sup> we estimate ( $20/44 \times 184.4/83.7 \times 12 =$ ) 12 bursts or ( $20/110 \times 184.4/83.7 \times 12 =$ ) 4.8 bursts to occur in our data. Based on the later reports<sup>3,4</sup> we estimate between ( $20/114 \times 184.4/83.0 \times 20 =$ ) 7.8 and ( $20/650 \times 184.4/83.0 \times 20 =$ ) 1.4 bursts on average in our experiment during the warmup period.

In the above estimate we made the reasonable assump-

tion that the burst is spread over a time scale shorter than our gate duration (of minimum 20  $\mu$ sec). In Ref. 2 evidence is suggested of the burst being instantaneous or of a duration exceedingly less than the gate duration ( $\Delta t \ll 50 \mu$ sec). This is concluded<sup>2</sup> by comparing the data to correlated neutrons emitted from a <sup>252</sup>Cf source with typical neutron multiplicity of 3–4. If, on the contrary, we assume that the burst is uniformly spread over the gate duration of 100  $\mu$ sec (as listed in Ref. 2) or 128  $\mu$ sec (as listed in Refs. 3 and 4) a correction factor should be added. For example, as discussed in Sec. II C for a burst of 130 (150) neutrons uniformly spread over 100  $\mu$ sec, our setup has a 48% (51%) chance of having a gate 80 (110)  $\mu$ sec long, see above. Note that half of the neutron bursts observed at Los Alamos included at least 120 neutrons. We then renormalize our overall observation efficiency by 0.44 (0.65) for detecting such extended bursts including approximately 130 neutrons [i.e., overall renormalization of 0.22 (0.325) for the expected burst rate]. In the Los Alamos experiment, due to the neutron die away time in their detector of 50  $\mu$ sec,<sup>3,4</sup> their detector would catch only 86% of a burst extended to 100  $\mu$ sec. This would then lead to the estimate of at least 1.2 and as many as 3 bursts in our data, based on the early data of Menlove *et al.*<sup>2</sup> and, on the average, between 0.4 and 2 bursts based on the later data of Menlove *et al.*<sup>3,4</sup>

While we discuss the effect of the gate width, we adopt the suggestion of Ref. 2 that the bursts are instantaneous, and in this case we expect between 4.8 and 12 bursts in our data based on the early data of Menlove *et al.*<sup>2</sup> We expect between 1.4 and 7.8 bursts based on the later data<sup>3,4</sup> of Menlove *et al.*

#### APPENDIX D: EXPERIMENTAL SYSTEMATICS

In the following we shall discuss possible improvements to our setup that may allow an increase of the sensitivity of our experiment, but do not invalidate our results (as suggested in Ref. 12) at the quoted level of sensitivity.

(1) Our detector system is designed to catch a small fraction of the burst. For example, for a burst of 100 neutrons, we show that we have at least 90% efficiency for detecting a 6, 7, 8, 9, or 10 fold event. Detection of a larger fraction of neutrons could be carried out via an increase in the number of detectors, but not by an increase in the individual detector efficiencies. An increase in the efficiency of each detector would increase the double hit probability (kept smaller than 4% in this experiment) and not allow for discriminating between a hit from a high-energy cosmic neutron and a simultaneous multiple hit of fusion neutrons summing to more than 2.45 MeV in the detector. We emphasize that such simultaneous hits cannot be resolved even via the use of multiple hit electronics owing to the finite time resolution (of a few tens of nsec) of such devices.

(2) Due to the low threshold used in this experiment, the gain of our detectors must be high, causing some of our detectors to saturate at energies greater than 4.4 MeV neutron energy. As we demonstrated above, the probability for such an occurrence in our data from a fusion event is smaller than 2%. Clearly this saturation

does not affect our experiment at the quoted level of sensitivity.

(3) Due to data read more than once in the buffer of the electronic module, MUX-PRW103, interfacing our Nuclear Data ND581 NIM ADC's to our CAMAC crate, cross talk was observed between different time-of-flight spectra. We emphasize that time-of-flight information is not used in any way to identify a burst and the cross talk does not interfere with our ability to demonstrate the occurrence of bursts. The cross talk disappears (to less than 1.5%) upon minimal pulse shape gating (i.e., requiring a pulse shape signal above threshold) in the appropriate

ADC channel as shown in Fig. 7. We note that all ten NIM ADC's are multiplexed and interfaced to the CAMAC crate via this single memory buffer. In addition, since the data in each ADC is read more than once, the clean time-of-flight spectrum for a given detector is reduced by a factor close to 2 with respect to the ungated data, as shown in Fig. 7.

(4) The time of flight between the two central detectors was not measured in this experiment. This fact does not affect our ability to search for bursts, since the signals from the two central detectors were timed with respect to each other so that hits in both detectors are included in

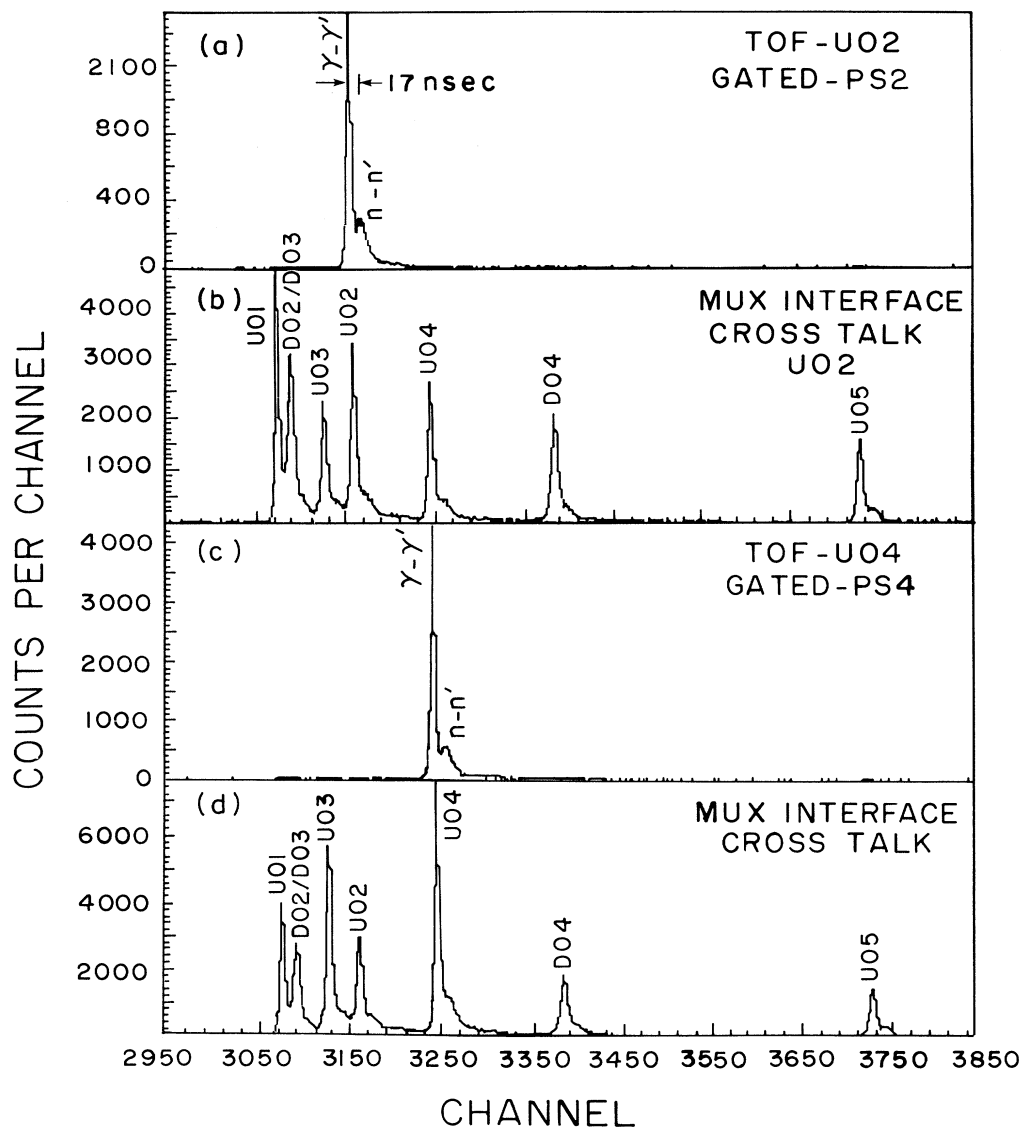


FIG. 7. Time-of-flight spectra obtained with a  $^{252}\text{Cf}$  neutron source; in (b) and (d) we show the cross talk discussed in Appendix D, part (3), and in (a) and (c) we show the clean spectra generated with minimal pulse shape gates.

the gate.

(5) For relatively small bursts ( $M < 100$ ) of duration exceeding  $20 \mu\text{sec}$ , an increase of the gate duration used in this experiment would be highly desirable. As de-

scribed above, for large bursts ( $M > 100$ ) our produced gate duration of  $20 \mu\text{sec}$  is extended to values as large as  $80 \mu\text{sec}$  or more and the short gate duration used in this experiment is not so crucial.

<sup>1</sup>S. E. Jones, E. Palmer, J. Czirr, D. Decker, G. Jensen, J. Thorne, S. Taylor, and J. Rafelski, *Nature* **338**, 737 (1989).

<sup>2</sup>H. O. Menlove, M. M. Fowler, E. Garcia, A. Mayer, M. C. Miller, R. R. Ryan, and S. E. Jones, Report LA-UR 89-1974 (unpublished); and S. E. Jones, private communication.

<sup>3</sup>H. O. Menlove, E. Garcia, and S. E. Jones, submitted to NSF/EPRI Workshop on Anomalous Effects in Deuterated Metals, Washington D.C., Oct. 16–18, 1989 (Report LA-UR 89-3633). We are indebted to R. L. Garwin for bringing this report to our attention.

<sup>4</sup>H. O. Menlove, E. Garcia, and S. E. Jones, submitted to DOE-ERAB panel on “cold fusion,” copy supplied to us by S. E. Jones.

<sup>5</sup>M. Gai, S. L. Rugari, R. H. France, B. J. Lund, Z. Zhao, A. J. Davenport, H. S. Isaacs, and K. G. Lynn, *Nature* **340**, 29 (1989).

<sup>6</sup>We are indebted to J. E. Hack of Yale University and J. R. Reilly of Brookhaven National Laboratory, for reviewing the procedures developed at Los Alamos for treating the Ti chips, and for bringing to our attention the problems associated with that treatment.

<sup>7</sup>Measured by J. R. Reilly at Brookhaven National Laboratory.

<sup>8</sup>J. P. Briand, G. Ban, M. Froment, M. Kaddam, and F. Abel, *Phys. Lett. A* (in press). We are indebted to J. R. Huizenga for bringing to our attention this paper.

<sup>9</sup>G. B. Hagemann *et al.*, *Nucl. Phys.* **A245**, 166 (1975).

<sup>10</sup>O. Anderson *et al.*, *Nucl. Phys.* **A295**, 163 (1978).

<sup>11</sup>L. Westerberg *et al.*, *Nucl. Instrum. Methods* **145**, 295 (1977).

<sup>12</sup>A. Anderson, private communication.

<sup>13</sup>S. L. Rugari, R. H. France, M. Gai, B. J. Lund, S. Smolen, Z. Zhao, S. E. Jones, K. W. Zilm, and K. G. Lynn, interim report submitted to the DOE/ERAB panel on “cold fusion,” Report Yale-3074-1037.

<sup>14</sup>W. Feller, *An Introduction to Probability Theory and its Applications*, 3rd. Ed (Wiley, New York, 1968), Vol. I, p. 59.

<sup>15</sup>S. E. Jones, as quoted in *Nature* **342**, 106 (1989).

<sup>16</sup>After the submission of this paper, a table was forwarded to us [Table III of a manuscript now published as H. O. Menlove, M. M. Fowler, E. Garcia, M. C. Miller, M. A. Paciotti, R. R. Ryan, and S. E. Jones, *Fusion Energy* **9**, 495 (1990)] containing an account of 9125 hours of data collection. While larger than our *lower limit* estimate of 5700 hours, this duration is still smaller than the 13 000 hour value quoted in Ref. 15.